Wear behaviour at 600°C of surface engineered low alloy steel containing TiC particles

A.N. Md Idriss[1],M.A. Maleque[1] ,I.I. Yaacob[1] ,R.M. Nasir[2] ,S. Mridha[3] and T.N. Baker[3*]

[1]Advance Manufacturing and Surface Engineering Research Unit

Department of Manufacturing and Materials Engineering

International Islamic University Malaysia

P.O. Box 50728, Kuala Lumpur, Malaysia.

[2]School of Mechanical Engineering, Universiti Sains Malaysia

Seri Ampangan, 14300, Nibong Tebal, Seberang Perai Selatan

Penang, Malaysia.

[3]Department of Mechanical and Aerospace Engineering

University of Strathclyde, Glasgow G1 1XJ, United Kingdom.

Email:[1]ahmednazrin@gmail.com; [1]maleque@iium.edu.my; [1]iskandar_yaacob@iium.edu.my;

[3]shahjahanmridha@gmail.com; [2]ramdziah@usm.my; [3*]neville.baker@strath.ac.uk

3*:Corresponding author.

Abstract

The aim of this work was to develop a surface that could resist wear at high temperatures, thus achieving a prolonged component life. Surface modification of a low alloy steel by incorporating TiC particles has been undertaken by melting the surface using a tungsten inert gas torch. The dry sliding wear behavior at 600°C of the original and modified surfaces was compared. Microscopic examination of both surfaces showed glazed layers across the wear tracks, with differing amounts of oxide and homogeneity. Extensive wear occurred on the low alloy steel surface, which showed deformation of the wear scar tracks, and a steadily increased friction coefficient. TiC addition reduced the wear loss, coinciding with a glazed layer 33% thinner than that on the low alloy steel sample.

Keywords: Tungsten inert gas torch, low alloy steel, titanium carbide particles, single and multipass tracks, high temperature wear, dry sliding, oxide layer.

Introduction

The increasing demand for material for high temperature wear applications has concentrated attention on improving the surface properties, by modifying the surface composition of the substrate.[1-5] If the material used is below the required specification, the consequences may be devastating, as the operating system can easily lose the permissible tolerance, leading to malfunction. Several materials such as titanium alloys , aluminium alloys and carbon steels, are known for their proneness to severe wear, due to their reduction of hardness and strength from thermal softening effects, and require surface reinforcement, especially when operating at high temperatures.[1-7] To overcome these problems, the ubiquitous TIG technique that is cheap, flexible, and low in operating and maintenance costs, has been used to develop superior surfaces to the parent materials compared to the expensive and complex lasers or electron beam techniques.[6-12] Improving the wear resistance of alloys requires a significant knowledge of the material to be surface

engineered and how the chosen process controls the microstructure of the modified surface. Research shows diverse results on oxidation, and the mechanisms that reduce this at high temperature. Chen and Wang[13] observed that TiC, mixed with an FeAl binder and laser clad, reduced wear severity at 400°C and 600°C, compared with a highly deformed and ploughed unreinforced austenitic stainless steel. It was found by Fontalvo and Mitterer[14], that additions of silicon and aluminum to steel reduced the oxide film thickness, resulting in an increase in the wear rate, especially at high temperatures. Transfer of material from the counterface used in wear testing, to form a compacted glaze, is well established.[15] For example, transfer occurred during testing a TiC-Fe surface at 250°C under a load of 520 N, but did not occur with the unreinforced pin. Also, increasing the TiC content in the surface, increased the wear rate, which became significant between 600°C and 800°C.[16] At room temperature, the debris was in the form of powder, while at 500°C the powders were compacted.[17] The load bearing areas were well burnished, with more oxide occurring in the middle of the wear track at 250°C, but less at 150°C and 20°C.[18] Others have also demonstrated that the oxide formed on the wear tracks is necessary to reduce the wear rate. [19, 20]

The current research considered TiC particulates in the size range 45 – 100 μm, melted into the surface of an AISI 4340 low alloy steel using the TIG technique. At room temperature, it has been shown that the wear resistance of a re-solidified zone, incorporating TiC particles, was 21 times greater than that of the unmodified low alloy steel substrate.[21] This is a relevant justification for further investigation to consider the wear resistance of this system at 600°C. Here, the wear behaviour at this temperature is compared to the untreated AISI 4340 low alloy steel substrate. The results from this investigation could be beneficial for high temperature applications particularly in the automotive, aeronautical or aerospace industries.

Experimental

An AISI 4340 low alloy steel, composition, 0.4C- 0.7Mn- 0.20Si-0.04S- 0.035P-0.8Cr- 1.65Ni-0.20Mo, remainder Fe (all wt.%) was cleaned with ethyl alcohol, and TiC particulates, 45 – 100 μm

in size, after mixing with a PVA binder, were preplaced at 1 mg mm^{-2} on the steel surface. The sample preparation prior to the TIG melting process to produce the single and multi-pass tracks, is described in previous publications.[6-11] In single track melting, the TIG torch was scanned over the preplaced powder as shown in Fig. 1, while for multi-pass track processing, which is necessary to cover an area, each track was overlapped by 50 %.

The single and multi-tracks were melted using an energy input of 1344 J mm^{-1} (30V; 85A) and shielded by argon delivered at 20 l min^{-1}. Equation 1 was used to calculate the energy input, where V and I are the voltage and current respectively, while s is the speed of the travelling TIG torch in melting a track across the preplaced powder sample. ɳ is the efficiency of the amount of absorbed energy in the sample, and this had been described elsewhere as 48%.[6, 22]

$$Energy\ Input = \eta \frac{VI}{S} \quad (1)$$

After melting and prior to wear testing, the multipass track specimens were ground to reduce the surface roughness by removing 0.4 mm from the surface. The dry sliding wear test conditions were set at a velocity of 3.46 cm s^{-1} and a load of 10 N, while a 6 mm dia. alumina ball was used as the counterface on a 5mm track radius. The sample was gradually heated by the test machine and the temperature detected by a sensor, as shown in Fig. 2. The machine must reach 700°C for the sample to attain a test temperature of 600°C. Boron was dusted onto the sample holder, to prevent any permanent adherence to the sample. The volume loss of the glaze layer (V_{loss}) was calculated by equation 2, which was previously used to assess the wear at room temperature; [20] W is described as width of the wear track and R is the radius of the alumina ball, while D is the track radius. The volume of oxide on the wear tracks was calculated using equation 3; the total loss ($V_{total\ loss}$) is the volume of material loss minus that of glaze layers.

$$V_{loss} = \frac{\pi}{6} \times D \times \frac{W^3}{R} \quad (2)$$

$$V_{oxide} = V_{total\ loss} - V_{loss} \quad (3)$$

Microstructural examination, to understand the mode of surface failure following wear testing, was undertaken with a JEOL 5600 scanning electron microscope. An Alicona Infinite profilometer was used to measure the geometric profile of the wear tracks, while a Wilson Wolpert hardness testing machine was used to measure the sample hardness under a load of 500 g_f, with a 10s indentation delay.

Results and Discussion

Figures 3 and 4 show the concave shape of the melt pool, with a relatively homogeneous distribution of TiC that is mixed between undissolved (here described as particulates), and partially dissolved and agglomerated TiC precipitate particles. Undissolved TiC particulates, remaining from the preplaced powder, are present due to poor heat absorption during melting. However, when the temperature exceeded the melting point of TiC, ~3200^{o}C, the particulates melted, and on cooling precipitated in the form of either flower, globular or dendritic types of TiC morphologies, Fig.4. No cracks were found in the resolidifed zone. The hardness of ≤1100 HV, was approximately four times the 300 HV hardness of the steel substrate. The achievement of this high hardness zone was due to the development of the a relatively homogeneous distribution throughout the melt zone,of both TiC particulates and smaller TiC precipitates. This was a result obtained from a series of trials using different amounts of preplaced powder with different energy inputs.

The Gaussian energy distribution of the TIG torch that determines the heat intensity for narrow melt depths, generates more melt in the centre and is gradually depleted towards the edges.[6-12] Therefore, when making use of this energy distribution for fabricating a surface area through multipass

tracking, each single melt track was overlapped 50% by the next track. This additional energy input, when covering a surface by multipassing, allows many of the partially melted TiC particulates still present after single track processing, Fig.3, to further or completely dissolve. On cooling the work piece, TiC, having different shapes and sizes, precipitates, Fig.4, a feature of the multitrack melt zone, whereas the single track microstructure is dominated by undissolved and partially dissolved particulate. This is a different situation from powder injection methods under fusion, where the overlapped layers receive an equal volume of reinforcing material.[23,24] In previous work, the processing to produce many overlapping tracks generated heat within the substrate that was valuable for reducing the solidification rate whilst refining the TiC microstructures.[10,11] Absence of preheating in the single track, which develops in overlapping tracks, resulted a higher solidification rate, and this reduced the extent of TiC particulate dissolution, leaving a significant volume near the melt-matrix interphase, Fig. 3. The increased melt volume produced by overlapping reduced the TiC concentration, resulting in the development of a lower melt zone hardness compared to a single track melt.

The inset in Fig. 4 shows TiC precipitates in the form of globular and flower morphologies within the 1 mm deep multipass tracks. The lower density of the TiC particulate, 4.93 g cm^{-3}, compared to the low alloy steel, 7.85 g cm^{-3}, resulted in the TiC floating and segregating near the surface. However,Maragonian forces redistributed the TiC particulates and precipitates, and depending on the viscosity of the melt, a longer solidification time in the middle zone of the melt track produced a higher volume of TiC precipitates. The centre region of the TIG arc generates more heat than the outer regions, producing higher temperatures in the middle zone of melt track, which resulted in a greater dissolution of the TiC particulates, resulting in more TiC precipitates.

Following the sliding wear tests conducted at 600°C, surface failures of the untreated and TiC treated samples, together with EDX spectra, are shown in Figs. 5 and 6 respectively. The EDX spectrum collected after the wear test, Fig.6, shows peaks of iron, titanium, oxygen. Aluminium was

not detected on the surface of any wear tracks, and this is a clear indication of the absence of material transfer from the alumina ball to the surface of the 'mechanically made alloy glaze' surfaces. The presence of the oxygen peaks in both samples, Fig.5 and 6, indicates that the iron is present as oxide. In previous work, the generation of heat by friction, during the wear testing at room temperature, was low, but sufficient to produce a glaze layer on the untreated sample.[21] However, the microstructure of the cross-sectioned room temperature samples observed by SEM showed no morphological signs of a visible glaze.[21] In the current work, testing at 600°C resulted in a higher rate of oxidation, and the development of an evenly distributed glaze on both untreated and TiC modified samples, Fig Z.

As the steel softened upon heating at 600^0C, the untreated sample, seen in Fig. 5, exhibited a relocation of material, in the form of large adherent transfer particles or straps, which are caused by deformation at the asperity contacts. These large adherences symbolize the load bearing capacity evident from the very smooth surface on each spot, as the materials are smeared and depressed. The abrasive wear noted in the steel with the TiC modified surface, Fig. 6, is the mechanism which sustains the burnished or polished surface, with negligible transfer of material to the wear track, compared to the adhesive wear observed in the untreated steel surface. Under these circumstances, the load bearing capacity that is borne by the surface engineered steel, is evenly distributed, with a reduction of the contact stresses on the wear track, thus hindering the possibility of surface infringement or glaze detachment. Both untreated and TiC surface modified samples are subjected to the depletion and regrowth of the oxide layers. Regrowth is associated with an increase of oxide or glaze thickness, which makes them susceptible to spallation upon subsequent contact with asperities.[20,25, 26]

Distributions of wear debris and characteristics of the ploughing grooves are different in untreated and TiC treated samples. The presence of wider ploughing grooves on the wear track with a large number of debris in Fig. 5, confirms that the substrate (untreated sample) has severe abrasive and

adhesive wear.

Cross-sections of both the samples seen in Fig.7, show glaze layers that are formed on the surface of the samples. For the untreated sample, the thickness of the glaze is 7.4 μm while that of the TiC surface modified sample is lower, at 5 μm. The incorporation of TiC particulates into the molten zone of the low alloy steel mitigates the formation of the glaze oxide at this high temperature, because iron has greater tendency to oxidize than titanium carbide. The glaze on the untreated sample, Fig.7a, demonstrates the unevenness of the surface (white arrows), which is due to deformation, with many adherent straps, Fig. 5. Unevenness of top surface of the glaze on the untreated sample indicated the high wear severity, which occurred during the wear process. This was unlike the surface modified by incorporation of TiC particulates and particles, where the glaze is relatively flat, Fig.7b, due to a well distributed load bearing capacity.

The glaze-substrate interphase in Fig. 7 exhibited an unevenness at the sample surface (black arrows), which occurred during the earliest stage of wear in the development of the glaze layers. It is envisaged that both untreated and TiC incorporated samples experience 'metal-to-metal' contact. This generated severe wear until well developed and adherent glazes were established. Because of the lower roughness of the TiC modified sample surface, the wear may have been halted in the midst of the wear process, which is clearly evident from the dominance of early stage interphase waviness.

The tribo powders (debris) taken from the wear surface of untreated sample, shown in Fig. 8, are comprised of solid pieces $\leq$ 400 μm × 220 and others <100 μm. When tribo powders, particularly those with larger sizes, are not well synthesized, fatigue stresses can initiate cracks, which propagate underneath the glaze, and are manifested by ripples. As the cracks progresses, the glaze loses its adherence to the surface of the track, which results in either glaze detachment, or incorporation into subsequent glaze layers. The larger tribo powders may have delaminated in the latter process or be otherwise crushed into smaller pieces. It has been shown that the severity of the adhesive wear is

strongly related to the size of tribo-powders.[27, 28] This present observations agrees with this opinion in the case of the untreated sample.

Figure 9 shows the surface profile of the wear track, while Fig. 10 presents the wear loss and surface oxidation for both the untreated and TiC incorporated samples. Fig.9a demonstrates that a greater penetration by the alumina ball occurred in the untreated sample, with the measured track depth and width being 33 µm and 920 µm, respectively. The corresponding data for the sample processed with TiC powder, are depth 25 µm and width 850 µm, see Fig. 9b. Using these data in equation 2, the track volume loss was calculated to be 0.678 mm^3 for untreated sample and 0.535 mm^3 for the TiC modified sample. The wear test was continued for 240 mins. for both samples. The wear rates were calculated for the untreated and the TiC modified samples as 283×10^{-5} mm^3 min^{-1} and 223×10^{-5} mm^3 min^{-1} respectively, which shows that wear rate is about 1.3 times faster in the untreated sample compared to the TiC modified sample. In other words, surface modification has reduced wear by 21% at 600^0C. This reduction is related to higher hardness value developed due to TiC incorporation. During the 240 mins. of wear testing, the oxide layer of the untreated sample was 7.4 µm thick, corresponding to a total oxide volume of 0.0335 mm^3,determined using equations 2 and 3. Similarly, for the TiC modified sample, with an oxide thickness of 5 µm, the total oxide volume formed is 0.0185 mm^3, which is 55% less than that of the untreated sample.

If it is considered that the oxide layer produced during the wear test remained adhered/embedded without significant loss by the wear test , the calculated oxidation rates for the untreated and modified samples are 14×10^{-5} mm^3 min^{-1} and 8×10^{-5} mm^3 min^{-1}, respectively. This oxidation rate is 1.5 faster in the untreated sample than in the modified sample, i.e., oxidation rate is 43% less in the modified sample. These results clearly suggest that incorporating TiC powder into the surface of the low alloy steel not only reduced the oxidation rate by 43% but also increased surface protection against wear by 21%. It is considered that TiC particles in the surface layer created an obstruction to oxygen diffusion into the steel surface, while the untreated sample had no

such barrier and generated more oxide. This can be a possible reason why the untreated sample produced an oxide layer nearly 1.5 times thicker than that of the treated sample. It is more likely that a continuous layer of TiC or higher concentration of TiC particles in the modified layer will further reduce oxidation. Higher concentrations of TiC particles may generate higher hardness and hence further reduce the wear rate.

Figures 11 and 12 show the variation of the coefficient of friction, μ, as a function of travelling distance and temperature for the untreated and TiC modified samples, respectively. The wear machine temperature was set at 700°C, which produced a sample temperature of 600°C. During the break-in period of 50m, μ increases to 5.5, Fig.11 and 4, Fig. 12.This is due to the various wear processes which built contact conformity, involving the alumina ball and the test samples, and when sample temperature was raised 250^0C a relative smoother surface then formed,[29] giving a coefficient of friction of 0.2. When the temperature of the samples attained 600^0C 100m. This phenomenon is different from the previous work at room temperature, where steady state μ was established after 100 m.[21] However for wear test at ~~For both samples, heated to~~ 250°C, these steady state trends are initiated at 0.2μ for both untreated and TiC modified samples after travelling for 50 m.[29] Heating ~~to 600°C~~ accelerates the rate of oxidation, which is the reason for the reduction in the earlier severe wear compared to that at the room temperature. The oxidation helps to build contact conformity for a steady wear trend.

The gradual increase in μ from 0.2 to 0.34 in Fig. 11 for the untreated sample, is associated with the relative steady rise in frictional resistance. Wear transitions are not observed in Fig. 11, which explains the continuous material removal as the counterface plunges deeper into the softened steel due to adhesive and abrasive wear while forming the glaze, Figs. 5 and 7. A similar trend in wear also dominated the TiC modified sample, with the steady rise of μ from 0.2 at 50 m, to 0.3 at 300 m. The coefficient of friction remains steady at 0.3 until the worn distance reaches 500 m. When the

wear rate surpasses the oxidation rate during the formation of glaze layer, embedding of the oxide straps is inevitable, as has been demonstrated by material failures.[18] Similar damage to the surface of the untreated sample is observed in this work, Figs 5 and 7a. However, when the oxidation rate is balanced by the wear rate, which occurred under mild wear conditions from μ of 0.3 at 300 m of the TiC modified sample, a burnished surface is observed, Fig.7b. Unlike severe wear that had shown deep wear grooves, mild wear is associated with less material loss.[21] Because of this, the wear loss for the TiC modified layer is minimal, based on evidence of a steady coefficient friction within the second half of wear process reaching 500 m. In the early stages of testing, both samples encountered severe wear, as seen from the increase in the coefficient of friction, Figs. 11 and 12. This explains why the severe-to-mild wear transition for the TiC modified sample, results in a two wear mode: the beginning is dominated by adhesive and abrasive wear, giving a steady rise in frictional resistance. This is followed, after 300 m, by abrasive dominated wear, which persists to the end of testing at a constant friction coefficient of 0.3. The incorporation of TiC into the melt zone provides a remarkable surface ability of reducing friction slightly below that of the untreated sample during the second half of the wear test, while in the process of undergoing surface burnishing. In the previous work at room temperature, the TiC modified layer had higher friction coefficient than the untreated low alloy steel.[21] The variation in the coefficient of friction is the clue to the wear or material degradation mechanisms and avoids misinterpretation of considering this as a single failure mode.

Conclusions

The single and multipass melt tracks incorporating TiC particulates studied in our previous research demonstrated that the resolidified melt zones have the potential for developing superior room temperature wear resistance. In the present work, wear testing at 600°C of samples containing TiC particulates incorporated into AISI 4340 low alloy steel samples, showed a decreased in oxidation rate by 43% together with 21% reduction in wear loss compared with the untreated steel. The higher wear rate in the untreated sample is associated with the appearance of a corrugated /wavy top

surface and a glaze-substrate interphase. These features are absent in the TiC treated sample, which shows a flat surface, associated with a lower wear rate. Different wear mechanisms for the two samples influenced the trends shown by the coefficient of friction, resulting in the different wear behavior of the untreated and TiC incorporated samples.

Acknowledgement

The authors would like to thank the Research Management Center (RMC) of International Islamic University Malaysia for funding this project under Research Matching Grant RMGS 12-007-0020.

Reference

1. J.D. Ayers: 'Particulate composite surfaces by laser processing', in 'Laser in Metallurgy', (ed. K. Mukherjee and J. Majumder), 115-125; 1981, Warrendale, Pennyslvania, Metallugical Society of AIME.
2. J.R. Stephens: 'Intermetallic and ceramic matrix composites for 815 to 1370°C (1500 to 2500 °F) gas turbine engine application', Tech. Memo., 102326, NASA, California, USA, 1990, 1-9.
3. S.Mridha and T.N.Baker; 'Metal matrix composite layers formed by laser processing of commercial purity Ti-SiCp in nitrogen environment', *Mater. Sci. Technol*., 1996, **12**,595-602.
4. Y. Terauchi, H. Nadano, M. Kohno and Y. Nakamoto: 'Scoring resistance of TiC- and TiN-coated gears', *Tribo. Int*., 1987, **20**, 248-254.
5. A.A. Howe: 'Wear resistant steel', *Mater. Sci. Technol*., 2016, **32**, 255-256.
6. S. Mridha, A.N. Md Idriss and T.N. Baker: 'Incorporation of TiC particles on AISI 4340 low alloy steel surfaces via tungsten inert gas arc melting', *Adv. Mat. Res*., 2012, **445**, 655-660.
7. S. Mridha, N.I. Taib and A.N. Md Idriss: 'Composite coating on steel surfaces by adding TiC and h-BN particulates under TIG torch melting', *Adv. Mat. Res.*, 2012, **576**, 463-466.

8. A.N. Md Idriss and S. Mridha: 'Microstructure of TIG melted composite coating produced using 1.0 and 1.5 mg/mm^2 TiC at an energy input of 2640 J/mm', *Adv. Mat. Res.*, 2012, **576**, 467-470.

9. S. Mridha, A.N. Md Idriss, M.A. Maleque, Suryanto and A. Souad: 'Effect of voltage on the consolidation of TiC particulates on steel substrate fused by TIG welding arc', *Int. J. Mech. Mater. Eng.*, 2012, **7**, 48-53.

10. S. Mridha and T.N. Baker: 'Overlapping tracks processed by TIG melting TiC preplaced powder on low alloy steel surfaces: *Mater. Sci. Tech*: 2015, **31**, 355-360.

11. S. Mridha, A.N. Md Idriss, M.A. Maleque, I.I. Yaacob and T.N. Baker: 'Melting of multipass surface tracks in steel incorporating titanium carbide powders', *Mat. Sci. Technol.*, 2015, **31**, 1362 -1369.

12. P. Muñoz Escalona, S. Mridha and T.N. Baker: 'Effect of shielding gas on the properties and microstructure of melted steel surface using a TIG torch', *Adv. Mat. Proc. Technol.*, 2015, **1**, 435 – 443.

13. Y.Chen and H.M Wang: 'High-temperature wear resistance of a laser clad TiC reinforced FeAl in situ composite coating', *Surf. Coat. Technol.*, 2004, **179**, 252-256.

14. G.A. Fontalvo and C. Mitterer: 'The effect of oxide-forming alloying elements on the high temperature wear of a hot work steel', *Wear*, 2005, **258**, 1491-1499.

15. C.C. Degnan, P.H. Shipway, J.V. Wood: 'Elevated temperature sliding wear behavior of TiC-reinforced steel matrix composites', *Wear*, 2001, **251**, 1444-1451.

16. X. Zhang, J. Ma, L. Fu, S. Zhu, F. Li, J. Yang, W. Liu: 'High temperature wear resistance of Fe-28Al-5Cr alloy and its composites reinforced by TiC', *Tribo. Int.*, 2013, **61**, 48-55.

17. I.A. Inman, S. Datta, H.L. Du, J.S. Burnell-Gray and Q. Luo: 'Microscopy of glazed layers formed during high temperature sliding wear at 750^{o}C', *Wear*, 2003, **254**, 461-467.

18. J. Jaren, F.H. Stott and M.M Stack: 'The role of triboparticulates in dry sliding wear', *Tribo. Int.*, 1998, **31**, 245-256.

19. I.I Garbar: 'Gradation of oxidational wear of metals', *Tribo. Int.*, 2002, **35**, 749-755.

20. G. Rasool and M.M. Stack: 'Wear maps for TiC composite based coatings deposited on 303 stainless steel', *Tribo. Int.*, 2014, **74**, 93-102.

21. A.N. Md Idriss, M.A. Maleque, I.I. Yaacob, R.M. Nasir, S. Mridha and T.N. Baker: 'Microstructural aspects of wear behavior of TiC coated low alloy steel', *Mat. Sci. Technol.*, 2016, **32**, 303-307.

22. K.E. Easterling: ‘Introduction to physical metallurgy of welding’, 1992, London, Butterworth-Heinemann.

23. M.F. Schneider: ‘Laser cladding with powder, effect of some machining parameters on clad properties’, PhD thesis, University of Twente, Enschede, The Netherlands, 1998.

24. R. Vilar: Laser cladding’, *J. Laser App.*, 1999, **11**, 64-79.

25. R.G. Bayer: ‘Mechanical wear and fundamental testing, 2nd edn, revised and expanded’, 2004, New York, Marcel Dekker Inc.

26. S. Kumar, A. Bhattacharyya, D.K. Mondal, K. Biswas and J. Maity: ‘Dry sliding wear behavior of medium carbon steel against an alumina disk’, *Wear*, 2011, **270**, 413-421.

27. E. Rabinowicz: ‘The least wear’, *Wear*, 1984, **100**, 533-541.

28. M.O. Alam, A.S.M.A. Haseeb: ‘Response of Ti-6Al-4V and Ti-24Al-11Nb alloys to dry sliding wear against hardened steel’, *Tribo. Int.*, 2002, **35**, 357-362.

29. A.N. Md Idriss: unpublished work.

List of Figures

Fig. 4: Melt pool of the multipass layers with more globular and flower precipitates at the top with fewer in the middle areas

Fig. 5: Surface failures of untreated sample at 600^{o}C with smooth surface on each adherent embedded strap (black arrows). Oxidation is indicated by the high oxygen peak in the EDX spectrum.

Fig. 6: Burnished surface with the TiC processed sample, tested at 600^{o}C. EDX spectrum shows a high oxygen peak which indicates oxide on the worn surface

Fig. 7: Cross sectional area showing glazes with (a) untreated that has embedded adherent straps, arrowed, with a deformed surface and (b) of TiC incorporated sample that is burnished on the top layer.

Fig. 8: Mixed shapes and sizes of tribo powders (debris) on the untreated samples surface. The largest is indicated by arrow.

Fig. 9: Wear profile of (a) the untreated sample that is larger in size compared to (b) the TiC modified sample.

Fig. 10: (a) wear loss and (b) surface oxidation for the untreated and TiC incorporated samples.

Fig. 11: Friction coefficient behavior of the untreated sample plotted against travelling distance and temperature. The gradual wear loss corresponds to an incremental rise in the coefficient of friction

Fig. 12: Friction coefficient behavior of the TiC modified sample as a function of travelling distance and temperature. The steady state coefficient of friction is attained after 300m, indicating a negligible wear loss

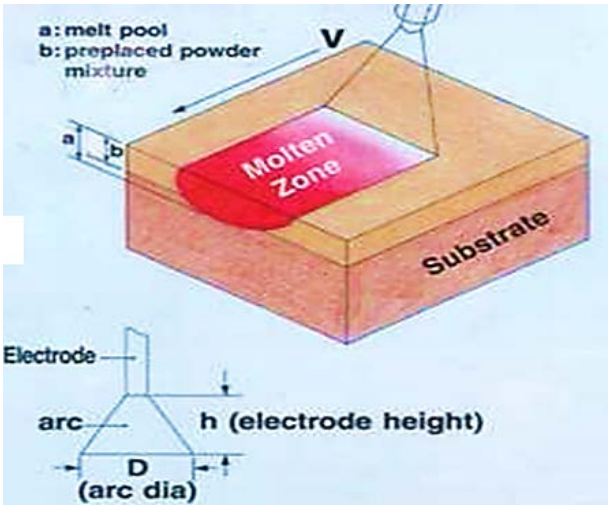
a: melt pool
b: preplaced powder mixture
V
a
b
Molten Zone
Substrate
Electrode
arc
h (electrode height)
D
(arc dia)

Fig. 1:

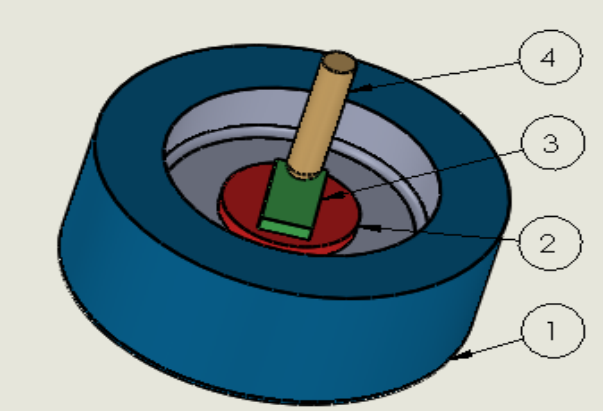

1	Machine	3	Sample
2	Holder	4	Sample sensor

Fig. 2:

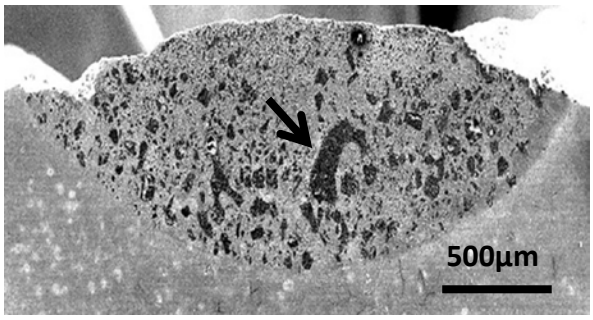

Fig. 3

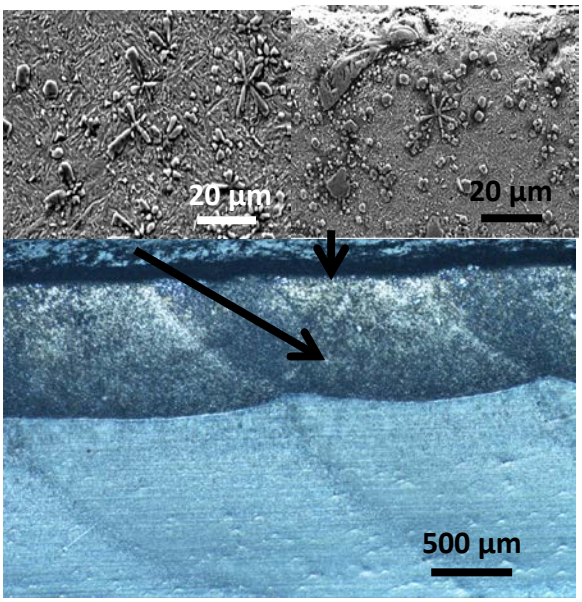

Fig. 4

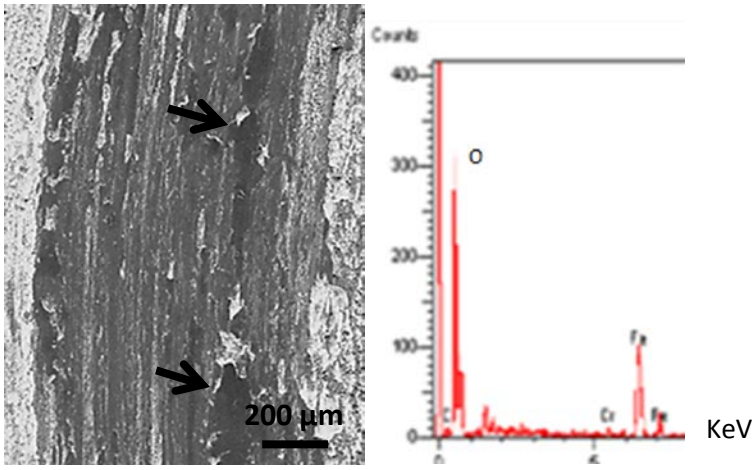

Fig. 5

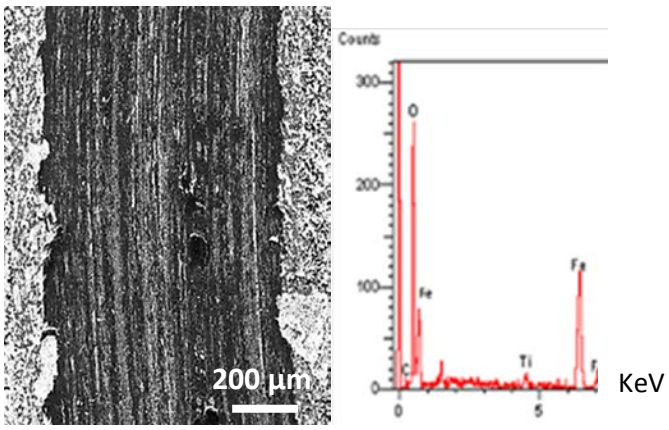

Fig. 6

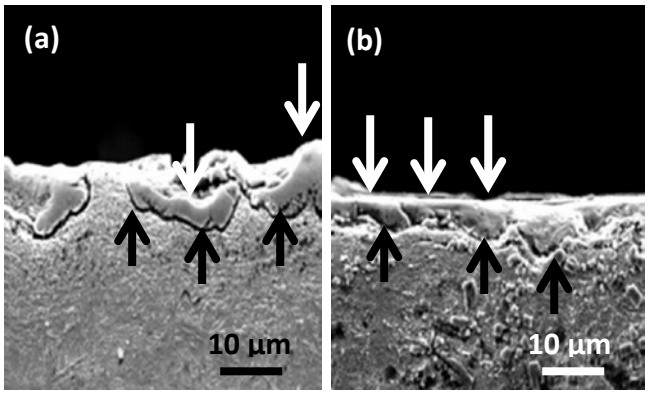

Fig. 7

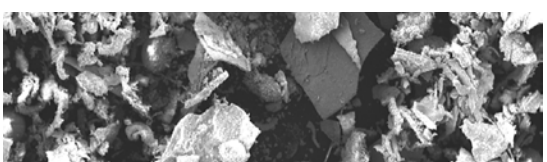

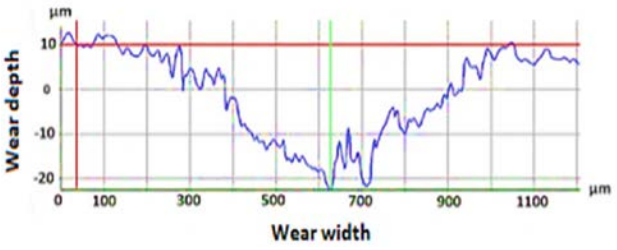
µm
10
0
-10
-20
Wear depth
0
100
300
500
700
900
1100
µm
Wear width

(a)

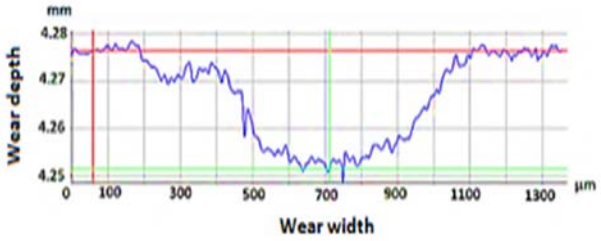
mm
4.28
4.27
4.26
4.25
Wear depth
0
100
300
500
700
900
1100
1300
µm
Wear width

(b)

Fig. 9

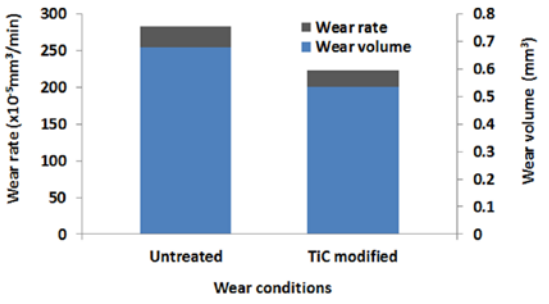
Wear rate (x10⁻⁵mm³/min)
300
250
200
150
100
50
0
Wear rate
Wear volume
0.8
0.7
0.6
0.5
0.4
0.3
0.2
0.1
0
Wear volume (mm³)
Untreated
TiC modified
Wear conditions

(a)

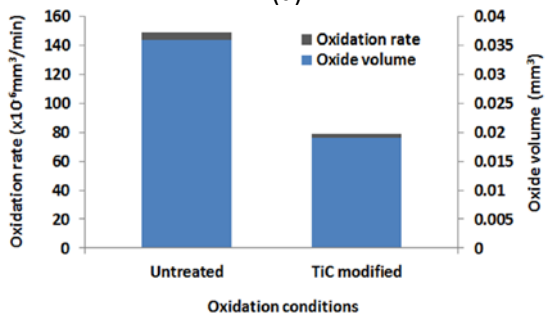
Oxidation rate (x10⁻⁵mm³/min)
160
140
120
100
80
60
40
20
0
Oxidation rate
Oxide volume
0.04
0.035
0.03
0.025
0.02
0.015
0.01
0.005
0
Oxide volume (mm³)
Untreated
TiC modified
Oxidation conditions

(b)

Fig. 10

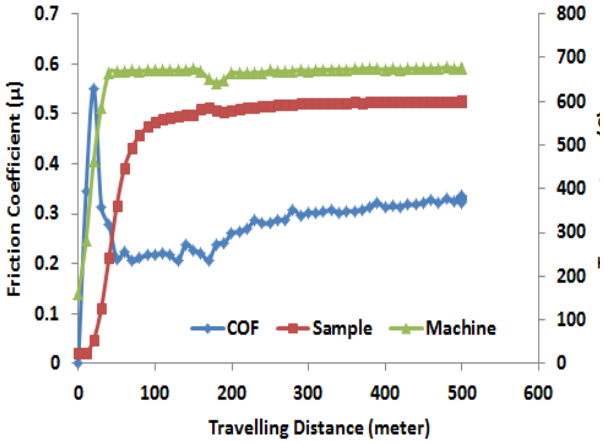
Friction Coefficient (μ)
0.7
0.6
0.5
0.4
0.3
0.2
0.1
0
800
700
600
500
400
300
200
100
0
0
100
200
300
400
500
600
Travelling Distance (meter)
COF
Sample
Machine

Fig. 11

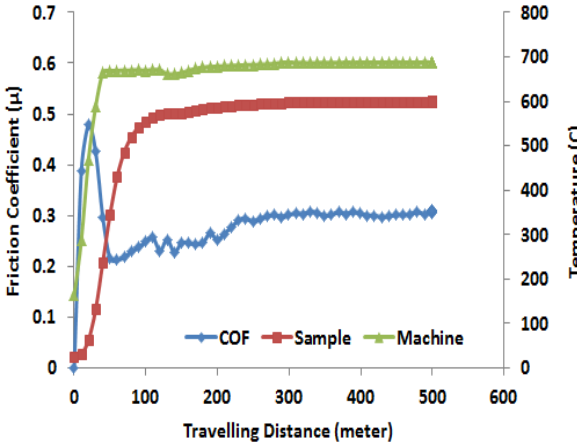

Fig. 12

The information below corresponds to the indicated alphabets in the above para.

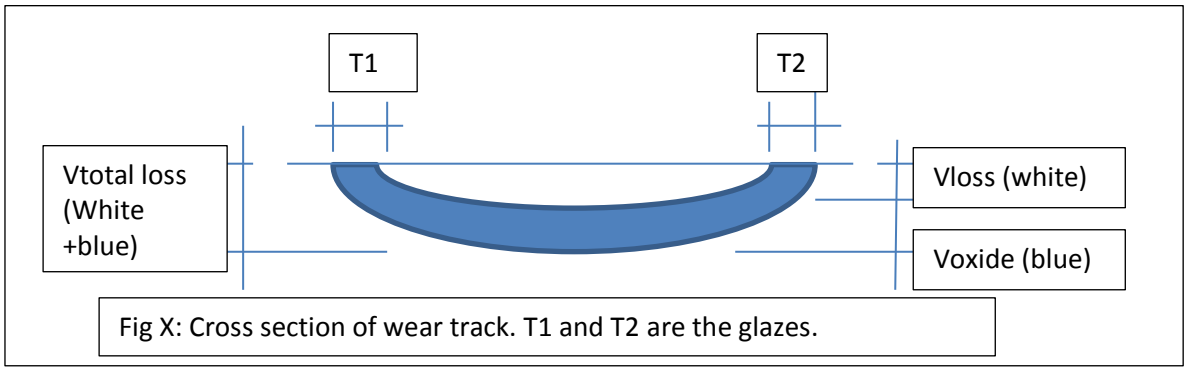

Fig X: Cross section of wear track. T1 and T2 are the glazes.

Untreated calculation

W = 0.92 mm D = 5 mm R = 3 mm; Total test time = 240 mins; T1 = T2 = 7.4 μm;

Substituting these values into Eqn 2;

Untreated V_{loss} = 0.678 mm^3 (A)

Untreated wear rate = 0.678/240 min = 283 x 10^{-5} mm^3/min (B)

Untreated Vtotal loss;

W = 0.935; Taking away the glaze layer by adding T1 and T2 (see Fig. X) .

Substituting the values into Eqn. 2;

Untreated Vtotal loss = 0.7138 mm^3

Using eqn. 3

Untreated Voxide = Untreated Vtotal loss – Untreated Vloss

= 0.03586 mm^3 (C)

Untreated oxidation rate = 0.03568 mm^3 / 240 mins = 149.43 x 10^{-6} mm^3/min (D)

TiC modified calculation

W = 0.85 mm D = 5 mm R = 3 mm; Total test time = 240 mins; T1 = T2 = 5 μm;

Substituting these values into Eqn 2;

TiC modified V_{loss} = 0.535 mm^3 (E)

TiC modified wear rate = 0.535/240 min = 223 x 10^{-5} mm^3/min (F)

TiC Modified Vtotal loss;

W = 0.86; Taking away the glaze layer by adding T1 and T2 (see Fig. A).

Substituting the values into Eqn. 2;

TiC modified Vtotal loss = 0.555 mm^3

Using eqn. 3

TiC modified Voxide = TiC modified Vtotal loss – TiC modified Vloss

= 0.019 mm^3 (G)

TiC modified oxidation rate = 0.019 mm^3/ 240 mins = 79.2 x 10^{-6} mm^3/min (H)

Therefore;

TiC modified V_{loss} = 0.535 mm^3; Untreated V_{loss} = 0.678 mm^3; TiC modified Voxide = 0.019 mm^3; Untreated Voxide = 0.03586 mm^3

0.535/0.678 = 0.79

(1 – 0.79) x 100 = 21% TiC modified protection

0.019/0.03586 = 0.55

(1-0.55) X 100 = 45% TiC glaze protection